Lighting up the cell surface with evanescent wave microscopy

Derek Toomre and Dietmar J. Manstein

Evanescent wave microscopy, also termed total internal reflection fluorescence microscopy (TIR-FM), has shed new light on important cellular processes taking place near the plasma membrane. For example, this technique can enable the direct observation of membrane fusion of synaptic vesicles and the movement of single molecules during signal transduction. There has been a recent surge in the popularity of this technique with the advent of green-fluorescent protein (GFP) as a fluorescent marker and new technical developments. These technical developments and some of the latest applications of TIR-FM are the subject of this review.

The old adage 'beauty is not skin deep' can be misleading. On the contrary, fascinating cellular processes, such as membrane docking and fusion can be revealed if one literally takes a more 'superficial' view. The specialized technique of evanescent wave or total internal reflection fluorescence microscopy (TIR-FM) specifically illuminates fluorophores in a thin optical plane on the coverslip and provides vertical resolution and signal-to-noise (S/N) ratio that is unmatched by any other light microscopy technique; even single fluorescent molecules can be observed and their dynamics and kinetics studied.

Recent developments in TIR-FM and related technologies are providing exciting new opportunities for exploring the cell and its molecules *in vivo* and *in vitro*. This review gives a brief description of TIR-FM, with emphasis on practical considerations, recent exciting applications (especially in vesicle fusion and single molecule detection) and a prediction of what lies ahead. Interested readers are encouraged to read some of the excellent in-depth reviews on TIR-FM theory[1], practical implementation[1,2], single molecules[3,4] and its other applications[1,5–7].

Derek Toomre*
Dietmar J. Manstein
Max Planck Institute for Medical Research, Dept of Biophysics, Jahnstrasse 29, D-69120 Heidelberg, Germany.
*e-mail: derek.toomre@mpimf-heidelberg.mpg.de
Future address: Dept of Cell Biology, Ludwig Institute for Cancer Research, Yale University School of Medicine, Stirling Hall of Medicine, 333 Cedar Street, PO Box 208002, New Haven, CT 06520-8002, USA.

What is total internal reflection?

The optical phenomenon of total internal reflection (TIR) can be observed in everyday life, from fibre optics to sparkling diamonds. The principle, based on Snell's law, is straightforward (Box 1): if light travelling in a dense medium (high refractive index, n_1) strikes a less dense medium (of lower refractive index, n_2) beyond a certain 'critical angle', θ_c, the light will undergo TIR. This critical angle depends on the relative refractive indexes of the two media. If the n_2/n_1 ratio is very small, such as occurs at an air–diamond interface (1.0/2.4), the critical angle is shallow ($\theta_c = 24.6°$) and TIR is easily achieved. Jewellers capitalize on this trick by cutting diamonds so that TIR occurs multiple times, 'trapping' the light before it refracts out of the top face.

Fluorescing footprints in the dark

Biologists, too, capitalize on TIR. In practice, cells are grown on glass coverslips or transparent materials of high refractive index (e.g. α-corundum – Al_2O_3), and a beam of light, usually from a laser, is optically coupled into the coverslip by a prism or the objective itself (Box 2). If light approaches the aqueous medium at $> \theta_c$, it totally reflects into the glass; however, if the light 'rays' (which are really electromagnetic wave fronts) simply bounced off the interface like a mirror, this would neither illuminate the cells, nor the biologists. In fact, at angles $> \theta_c$, some of the energy slightly penetrates the aqueous medium as an 'evanescent wave', propagating parallel to the interface due to 'near field' effects. This seemingly mysterious 'tunnelling' effect can be derived from Maxwell's equations on the behaviour of electromagnetic fields at a dielectric interface. Axelrod *et al.* explain the theory in detail[1] and interactive films are also available on the internet (see http://www-optics.unine.ch/research/microoptics/RigDiffraction/main.html and http://www.phy.ntnu.edu.tw/java/indexLayer.html#).

An important property of the evanescent wave is that the intensity falls off exponentially away from the coverslip (Box 1). The theoretical 'penetration depth' (the distance where the intensity has decreased to I_0/e) depends on the incidence angle, wavelength and polarization of light, as well as the refractive index of the coverslip and medium. Penetration depths of <100 nm are easily achieved. The net effect is that only fluorophores near the coverslip, corresponding to the 'footprint' of the cell, are excited; for this reason, one of the first applications of the technique was to monitor cell–substrate contacts (for reviews, see Refs 5 and 6).

Advantages of TIR-FM

It is the ability to make an optical slice with the dimensions of a thin electron microscopy (EM) section that lies at the heart of TIR-FM applications. How does this technique compare with much more familiar confocal systems? TIR-FM typically illuminates a vertical slice of <100 nm as opposed to a slice of ~500–800 nm for 1- and 2-photon confocal systems, respectively. This thin optical sectioning means that

http://tcb.trends.com 0962-8924/01/$ – see front matter PII: S0962-8924(01)02027-X

Box 1. Some key TIR formulas

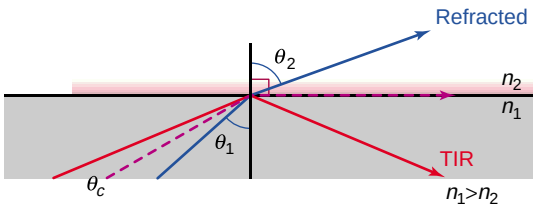

Fig. I. TRENDS in Cell Biology

Snell's law:

$$n_1 \sin\theta_1 = n_2 \sin\theta_2$$

θ = angle of incidence, n = refractive index

Critical angle:

At the critical angle, θ_c, $\theta_2 = 90°$; $\sin 90° = 1$;

$$n_1 \sin\theta_c = n_2$$

$$\theta_c = \sin^{-1}(n_2/n_1)$$

If $n_1 = 1.515$ and $n_2 = 1.36$, $\theta_c = \sin^{-1}\left(\frac{1.36}{1.515}\right) = 63.85°$

Evanescent field:

$$I_z = I_0 \exp^{-z/d_p}$$

$$d_p = \frac{\lambda}{4\pi\sqrt{n_1^2 \sin^2\theta_1 - n_2^2}}$$

I = intensity, z = distance, λ = wavelength,
d_p = penetration depth

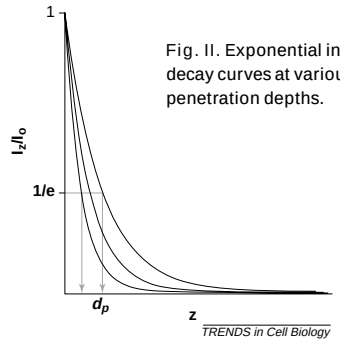

Fig. II. Exponential intensity decay curves at various penetration depths.

TRENDS in Cell Biology

the S/N ratio is much better than with confocal images, and cellular photodamage and photobleaching are minimal (but minimizing focal plane drift is also more crucial). TIR-FM images are captured frame-by-frame with charge-coupled device (CCD) cameras. These are sensitive and/or fast (but rarely both) and can now reach up to ~80% quantum efficiency and speeds of ~200 Hz (frames/s). Image intensifiers are required for single molecule sensitivity or can be used to minimize exposure times when imaging live cells. By contrast, most confocal systems scan the sample pixel-by-pixel, reject light with the pinhole and use photomultipliers. Generally, frame rates are slow (~0.1–5 Hz) and photon detection efficiency is relatively low. Nipkow disc-based confocal systems use video cameras for detection and can reach ~10-fold faster frame rates; however, the most important difference is that a confocal section is much thicker than an evanescent field.

But TIR-FM is not necessarily the panacea. Confocal microscopes can generate deep three-dimensional (3D) images of cells and photobleach areas of interest. Rather, TIR-FM is a complementary approach that can be combined with other microscopy techniques, such as brightfield, epifluorescence (EPI), confocal, fluorescence correlation spectroscopy (FCS), atomic force microscopy (AFM) and fluorescence lifetime imaging microscopy (FLIM), to mention a few[5]. TIR-FM is also compatible with fluorescence recovery after photobleaching (FRAP) and fluorescence resonance energy transfer (FRET) experiments[1].

The recent surge of reports using TIR-FM might create the impression that it is a brand new technique. In fact, the basic principles and approaches were described and applied in the early 1980s, championed largely by the efforts of Daniel Axelrod and other biophysicists[1]. So why the lag in its popular application to cell biology? First, looking at fluorescent markers in live cells was difficult until the recent advent of green fluorescent protein (GFP) and its cyan, yellow and red derivatives (CFP/YFP/DsRFP). Second, choosing and implementing a TIR-FM system, although not difficult, is not trivial either. In this regard, the recent introduction of new objective lenses, condensers and other materials affords greater opportunities.

TIR-FM practical considerations

Most TIR-FM set-ups are custom built and numerous configurations are possible[1]. The choices can be overwhelming. Does one need an inverted or upright microscope? Should one use mirrors or fibre optics to guide the light? Will the light be coupled through a prism or an objective ('prismless') type set-up? Unfortunately, there is no single 'right' solution; the optimal set-up depends on the needs of the user. Nevertheless, some rules and non-obvious issues should be borne in mind[2].

Basically, there are two major kinds of TIR-FM set-ups: prism- and objective-types (Box 2). Both systems typically use lasers for illumination. Collimated light is sent into a condenser via mirrors or an optical fibre; we prefer the latter as it is easier to implement and vibrations are less problematic. Of potential interest, TILL-Photonics (Martinsried, Germany) has recently developed a dual EPI/TIR condenser, compatible with Olympus objective-type set-ups. A major advantage of objective-type set-ups is that they allow imaging and concomitant manipulation of cells by patch-clamping,

Box 2. Two common TIR-FM set-ups

Cells are plated on coverslips (dashed black line; Fig. I) and placed in a chamber filled with dye-free medium or aqueous buffer. In the prism-type set-up (a) excitation light from a laser (green) strikes a prism (shown as a half-cylinder here) that is optically coupled to the coverslip by immersion oil or other liquid of matching refractive index (yellow). The decaying evanescent field illuminates the cells. Light emitted from the fluorophore (red arrow) is collected in a high NA water immersion lens. Note that access to the sample is partially blocked by the objective. In the objective-type set-up (b), there is full access to the cell. However, unlike the prism-type set-up, excitation light and emitted light are both collected by the objective and must be blocked by appropriate dichroic and emission filters (not shown). *NA = $n \sin\alpha$, where n is the refractive index of the medium between the object and the lens and α is half the intake angle of the lens.

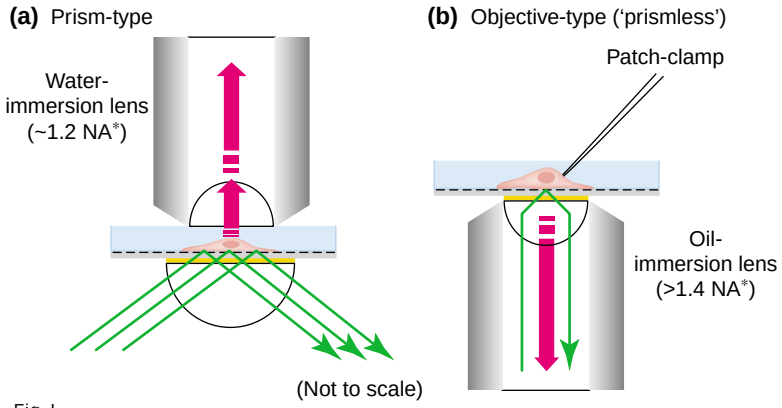

Fig. I.

TRENDS in Cell Biology

microinjection and other techniques. In prism-type set-ups, the water-immersion objective can hamper such manipulation, and in inverted microscopes, closed chambers must be used. Other advantages of objective-type set-ups are that more emitted light is detected and its intensity drops off monotonically with distance[1,2,7].

For prism-type set-ups, the incidence angle of the laser beam can be varied precisely over a wide range and the penetration depth is therefore well controlled. By contrast, with objective-type set-ups it is more difficult to control the angle of incidence precisely[8]. In fact, with standard high numerical aperture (NA) oil-immersion objectives, TIR is difficult to achieve at all. First, for TIR to occur, there must be a difference in refractive indexes. For objective-type set-ups, this means that the NA of the lens must be greater than the refractive index of the cell cytosol (1.36–1.38). With a 1.4 NA lens, only ~2.8% of the aperture (on the periphery) can be used for TIR[2]. In practice, the critical angle is just surpassed (~1.9° beyond); therefore, correctly coupling the laser into the objective is tricky. Better results are achieved with a new 1.65 NA lens from Olympus[7,9–11]. However, special high refractive index coverslips (which are expensive) and immersion oils (which are toxic) must be used. Lenses of 1.45 NA that are compatible with standard coverslips and immersion oils should be available soon from several manufacturers including Olympus and Zeiss. Importantly, these 1.45 and 1.65 NA objectives allow ~10% and ~25% of the aperture, respectively, to be used for TIR over a larger range of angles, which is a considerable improvement.

Observing vesicle fusion

There is an element of truth to the statement 'you have to see it to believe it'. This is perhaps best exemplified in the field of membrane trafficking and fusion. Hundreds of biochemical, genetic and EM experiments have indicated that regulated and constitutive vesicles traffic to, and fuse with, the plasma membrane. However, these approaches are, to varying degrees, indirect and cannot investigate the complex spatial–temporal dynamics of the process.

Patch-clamping was a technological breakthrough and opened the door for detecting changes in surface area (capacitance) or release of oxidative material with high temporal resolution[12]. From studies of regulated exocytosis in neuroendocrine cells and kinetic modelling, various pools of vesicles, including 'docked' and 'ready-releasable' pools were inferred. Although very powerful, the approach has its shortcomings; only the fusion event is monitored and prior vesicle trafficking, tethering and docking are not detected. Specificity is difficult as all fusion events are detected and most studies are therefore limited to regulated inducible exocytosis. There is also little spatial information on where exocytosis occurs. By contrast, EM has fantastic spatial resolution, but only gives 'snapshots' of the process.

TIR-FM offers an attractive compromise in that good spatial–temporal resolution can be achieved. Chromaffin cells are a good model system as they have the advantage of being generally well characterized and packed full of relatively large (~250 nm diameter) acidic granules that can be labelled with fluorescent acidotropic dyes. Almers and colleagues observed that, after a stimulus, granules fused with the plasma membrane and secreted dye into the medium as a bright 'puff' that could be detected by TIR-FM[13]. Simultaneous capacitance measurements and complementary EM studies confirmed that indeed granule fusion was specifically detected by TIR-FM[13]. Moreover, vesicles became exponentially brighter as they approached the plasma membrane and nanometre-sized vertical changes, caused by membrane docking, gave a large increase in fluorescence; an optical property unique to TIR-FM (but see caveats with prism-type set-ups[7,14]). Since Almers' TIR-FM study of exocytosis[13], a rapidly increasing number of TIR-FM studies with refined techniques have exploited this approach for monitoring regulated[8,11,14–20] and constitutive[10,21,22] exocytosis.

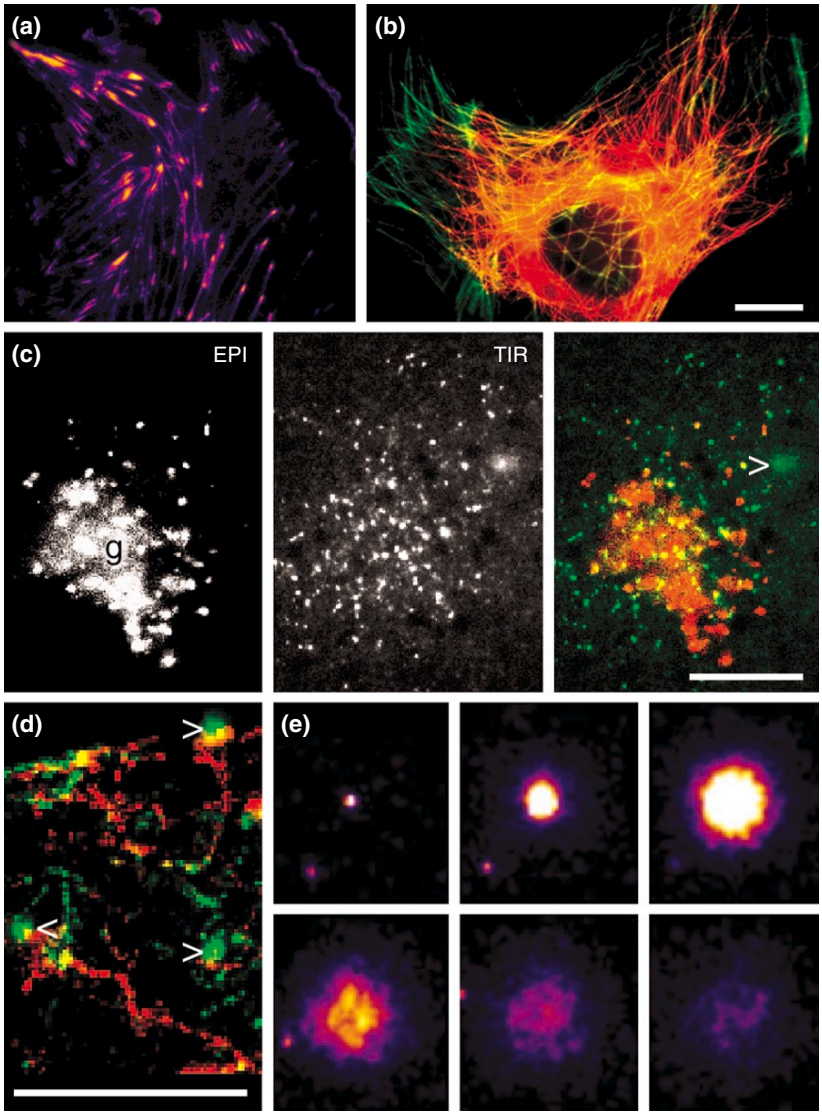

Fig. 1. Images of cell cytoskeleton and membrane traffic with TIR-FM. (a) and (b) are images of the TIR fluorescent signal that have been false coloured; bright to dimmest signal is white > yellow > red > purple. For b–d, the normal epifluorescent signal (EPI) is coloured red and the TIR fluorescent signal is shown in green. All images are from PtK_2 epithelial-like cells labelled with various YFP constructs. (a) Actin-YFP: note that the ends of stress fibres (likely to be focal adhesions) are particularly bright. (b) Tubulin-YFP. Tubulin near the coverslip is yellow-green. Note that single microtubules can be clearly observed by TIR-FM (green) even under dense areas of microtubules (red). (c) Different views of membrane cargo. VSVG-YFP (Ref. 21), a membrane protein, was accumulated in the Golgi (g) and then released. The cursor indicates a vesicle that has just fused with the plasma membrane. Note that the EPI and TIR images of the cell are very different (even though the focal plane was not changed). In EPI, the Golgi area is brightly stained, whereas in TIR vesicles near the plasma membrane are brightest; there is weak membrane staining due to VSVG-YFP that has already fused. (d) Tracking trafficking and fusion. A series of ~200 frames were back-subtracted and the difference image was projected. Vesicles that moved out gave a red EPI 'track', turned yellow-green as they approached the plasma membrane and fusion itself gave a green circular 'flash', indicated by the cursors. (e) Collage of a vesicle undergoing fusion. Starting at top left, 1 s intervals are shown from left to right. The fading of the signal in frames 4–6 is due to lateral diffusion of VSVG-YFP in the membrane. All images were taken with a prism-type TIR-FM microscope as described in Ref. 21. Scale bars in (a–d) are 5 μm, and boxes in (e) are 2 μm. Videos relating to this figure can be found at www.livingroomcell.com. Films of TIR-FM of vesicles and single molecules from several groups are available in the 'GFP in Motion 2' CD (supplement to *Trends in Cell Biology*). In addition, many of the primary articles in the reference list have accompanying films.

Exocytosis in action: kissing, hotspots and fusion

To give an overview of the potential of this technique, some major and unexpected findings from the aforementioned exocytosis studies are summarized. The first characteristic is that vesicles, whether granules, constitutive vesicles or synaptic vesicles, can be followed from where they first dimly appear in the evanescent field (~100–400 nm) until they fuse with the plasma membrane as bright flashes. Another feature of TIR-FM is that, in calibrated systems, fluorescence changes can be extrapolated to changes in axial position. This means that, although the cells are only imaged in two dimensions, 3D information on the position of vesicles can be obtained. One technical improvement has been the use of acousto-optical deflectors (AODs) to rapidly switch the incidence angle of the laser beam in prism-type set-ups[17,19]. The depth of the evanescent field can be quickly changed, allowing the vesicle to be tracked deeper in the cell and the position to be detected more accurately. However, on a cautionary note, scattering from within the cell causes the observed penetration depth, d_p, to be as much as 3.5-fold greater than theoretical calculations when d_p is >150 nm[8,17,19]. Another variation is to use dual shutters to switch rapidly between standard widefield EPI and TIR[21]. EPI provides a good overview of events near the plasma membrane and deeper in the cell, whereas TIR fluorescence selectively excites approximately the bottom 100 nm (see Fig. 1). When images of EPI and TIR were false coloured and merged, the entire sequence of late constitutive exocytosis – from cargo exit out of the Golgi, trafficking and fusion – could be followed[21] (Fig. 1d). There are other useful applications of AODs in TIR-FM; they can be used as ultra-fast shutters and can quickly change the excitation wavelength in systems equipped with multi-line lasers.

The tracking of vesicles has led to some surprising observations. Granules and synaptic vesicles were observed to approach the plasma membrane at an angle, presumably guided there by the cytoskeleton[8,14]. The lateral diffusion of granules and synaptic vesicles decreased approximately five fold when the granules 'docked' near the plasma membrane, suggesting restrictive diffusion, perhaps due to the cortical actin meshwork[8,13,14]. Interestingly, the 'priming time', or time taken to go from a morphologically docked to fused state, varied considerably (~0.25 s for synaptic vesicles[11], ~1 s for chromaffin granules[14] and ~40 s for constitutive vesicles[21]).

Other surprising discoveries were made. Many constitutive vesicles were 'docked', often for several minutes[21]. A significant fraction (>25%) of docked vesicles did not fuse and detached from the membrane[11,14,21]. A dual-colour study indicates that granules can 'kiss' the membrane and secrete soluble cargo yet retain membrane proteins associated with the granule, implying a 'kiss and glide' model[20]. Partial fusion from the tips of membrane tubules was also observed[21]. Also, when fusion events were positionally mapped,

Table 1. Spectral properties of selected fluorophores

Spectral property	Fluorophores				
	Cy3	Cy5	Alexa 532	Alexa 546	eGFP (S65T)
Max absorption λ_m (nm)	549	646	531	557	488
Max emission λ_e (nm)	573	670	554	572	508
Extinction coefficient, ε_m (M^{-1} cm^{-1})	150 000	218 000	80 000	98 000	55 000
Quantum yield Φ	0.33	0.28	0.95	~1.0	0.61
Rate of photobleaching at 10 MWm^{-2} (s^{-1})	0.007	0.4	0.06	~7 [0.07][a]	0.06
Total number of emitted photons/fluorophore $\times 10^6$	38	1.4	13	0.05 [5][a]	5

[a]Values in brackets refer to the rate of photobleaching and total number of emitted photons/fluorophore $\times 10^6$ at 1 MWm^{-2} (s^{-1}). We thank Michael Anson (NIMR, London, UK), who kindly provided the information for this table.

exocytic 'hot spots' were discovered in neurons[11], chromaffin cells[17] and epithelial-like PtK_2 cells[22] (although these were random in Cos-1 fibroblasts[10]).

These observations with TIR-FM allow new questions to be addressed. How are vesicles directed to these 'hot spots'? How are the kinetics of docking, priming and fusion modulated? Why do some vesicles escape fusion? Are there molecular kinetic 'timers' involved? The answers are not yet clear, but remember that these questions only resurfaced after TIR-FM results 'puffed', 'kissed' and 'flashed' in.

Observing single molecules with TIR-FM

An area that promises to give a great payoff is the monitoring of individual biomolecules in their natural environment in real time. Single chromophores, such as tetra-methyl-rhodamine, Alexa532 and Cy3 can be cycled repeatedly between their ground and excited electronic states to emit a sufficiently large number of photons for detection. Single molecule measurements can reveal events not detected by conventional, ensemble-averaged measurements such as rare conformational states, memory effects and molecular individualism. Single molecule detection using TIR-FM was successfully used for the characterization of molecular motors (e.g. Fig. 2). Landmark papers include the detection of individual ATP turnover reactions on myosin[23], and observation of binding and movement of single kinesin motors on microtubules[24].

A particular challenge in the motor field lies in the simultaneous detection of chemical and mechanical events at the single molecule level. Parameters such as the kinetics of motor–filament interactions, nucleotide binding, and how fast and far the motors move for each molecule of ATP hydrolysed need to be determined. In this context, a particular advantage of objective-type TIR-FM is that it can be easily combined with tools such as laser traps and AFM for mechanically manipulating biomolecules[4].

A vital aspect of visualizing single molecules is the S/N ratio; the better this ratio, the easier and more precise the detection will be. Because of the thin optical sectioning in TIR-FM, the background noise is dramatically reduced (being as much as 2000-fold lower than in conventional EPI microscopes[23]). In addition, for an adequate S/N ratio, stable, bright dyes that have high extinction coefficients, good quantum yields and are resistant to photobleaching are required. In this respect, sulphoindocyanine dyes (Cy3 and Cy5), sulphonated rhodamine dyes (Alexa532 and Alexa546) and enhanced GFP (eGFP) are suitable (Table 1). Other considerations are the actual properties of the fluorophore, such as its photobleaching rate, and, in the case of GFP, its tendency to 'blink'[3]. Additional factors that can affect the kinetic and spectral properties of the dye are the stereochemistry of the chromophore and its attachment to the ligand. It is crucial that the fluorescent substrate analogue is first shown to be homogeneous and behaves correctly at the macroscopic level before single molecule studies are undertaken. For studies of molecular motors, Cy3 analogues of ATP are advantageous in that they change their signal intensity in solution studies, but Alexa dyes do not. Subtle differences can be important. The 2′ and 3′ isomers of Cy3-EDA-ATP show kinetic behaviour similar to that of ATP in their interactions with myosin, but the two isomers display greatly different changes in fluorescence intensity upon binding to myosin[25].

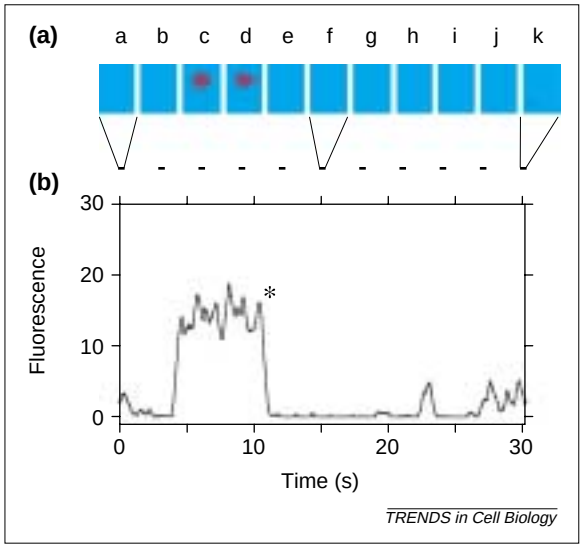

Fig. 2. Time series of a single Cy3-EDA-ATP molecule binding to a myosin filament as observed by prism-type TIR-FM. (a) Boxes (7 x 10 μm) show a rolling eight frame average taken at the time points indicated by the dashed lines underneath. Note that the bright signal in boxes c and d is due to the appearance of a single molecule. (b) The line trace is a time profile of the integrated fluorescence intensity of the boxed area. The rapid rise and fall is due to the binding and disappearance of a single Cy3-EDA-ATP molecule. The asterisk indicates either unbinding or photobleaching. To differentiate between Cy3-EDA-ATP release and photobleaching, laser power is typically varied to confirm that the observed rates are independent of the power density or photobleaching (not shown). These data were kindly supplied by Kazuhiro Oiwa and Michael Anson and are based on a prior study[25].

Clearly, in addition to showing where molecules are localized, the visualization of single molecules can offer detailed mechanistic information. In summary, ideal substrate analogues for single molecule studies need not only to be bright and stable but homogeneous and well characterized on the macroscopic level.

Future prospects

What does the future of TIR-FM hold for cell biologists? In our opinion, it will be pushed largely on two fronts: continuing technical advances and the application of TIR-FM to new areas of cell biology. One advance will be the continued merger of TIR-FM with other microscopy techniques such as FCS, AFM and FLIM. Another will be the ongoing development of dual- and multi-coloured TIR-FM so that multiple dyes can be observed in live cells. Two recent reports have used dual colour emission detection for dyes that can be excited at a single wavelength[20,26]; in principle, implementing TIR-FM with multiple excitation is also feasible. Improvements in the detection efficiency and speed of cameras as well as the properties of dyes will aid in single molecule detection. The application of fluorophores such as flavin nucleotide analogues and quantum dots for single molecule work offers exciting possibilities because of their unique optical properties and compatibility with biological systems.

A number of interesting applications are possible on the cellular front. Although most membrane trafficking studies have focused on exocytosis, studies of endocytosis with TIR-FM should be possible, and equally exciting. Although for brevity we have not focused on the cytoskeleton here, TIR-FM is clearly an elegant approach for specifically studying the cytoskeleton near the substrate (e.g. see the local illumination of actin and microtubules in Fig. 1). For instance, TIR-FM revealed that 'comet-like' actin tails, originating at the plasma membrane, propelled pinosomes into mast cells[27]. Molecular and genetic manipulation of cells, coupled with optical detection and analysis, will further extend the range of the approach.

The fact that many signalling events are initiated by recruitment and/or clustering of lipid rafts underscores the complex lipid and protein dynamics at the membrane[28]. Clearly, there is an enormous potential for using TIR-FM to study signal transduction[26,29]. For example, single Cy-labelled epidermal growth factor (EGF) molecules were detected by TIR-FM. Binding to the EGF receptor and subsequent dimerization of EGF caused spots to double in intensity and FRET to occur[26]. These two reports[26,29] are an exciting prelude of what we predict to be a growing field. There is no doubt that live imaging of cellular dynamics near the plasma membrane has a bright future – with evanescent wave technology it appears even brighter.

Acknowledgements
We thank K. Oiwa, M. Anson, A. Rohrbach, M. Oheim and P. Blattner for help and discussions. D.T. and D.J.M. were supported by the Max-Planck-Society and a grant from the Volkswagen-Stiftung. Owing to limited space, we apologize that only a subset of the primary articles are referenced.

References

1 Axelrod, D. *et al.* (1992) Total internal reflection fluorescence. In *Topics in Fluorescence Spectroscopy: Biochemical Applications* (Vol. 3) (Lakowiez, J., ed.), Plenum Press
2 Oheim, M. Imaging transmitter release. II. A practical guide to evanescent-wave imaging. *Lasers Med. Sci.* (in press)
3 Pierce, D. and Vale, R.D. (1999) Single-molecule fluorescence detection of green fluorescence protein and application to single-protein dynamics. *Methods Cell Biol.* 58, 49–73
4 Ishii, Y. and Yanagida, T. (2000) Single molecule detection in life science. *Single Mol.* 1, 5–16
5 Thompson, N.L. and Lagerholm, B.C. (1997). Total internal reflection fluorescence: applications in cellular biophysics. *Curr. Opin. Biotechnol.* 8, 58–64
6 Burmeister, J S. *et al.* (1998) Application of total internal reflection fluorescence microscopy to study cell adhesion to biomaterials. *Biomaterials* 19, 307–325
7 Steyer, J.A. and Almers, W. (2001) A real-time view of life within 100 nm of the plasma membrane. *Nat. Rev. Mol. Cell Biol.* 2, 268–275
8 Steyer, J.A. and Almers, W. (1999) Tracking single secretory granules in live chromaffin cells by evanescent-field fluorescence microscopy. *Biophys. J.* 76, 2262–2271
9. Terakawa, S. *et al.* (1997) Development of an objective lens with a high numerical aperture for light microscopy. *Bioimages* 5, 24
10 Schmoranzer, J. *et al.* (2000) Imaging constitutive exocytosis with total internal reflection fluorescence microscopy. *J. Cell Biol.* 149, 23–32
11 Zenisek, D. *et al.* (2000) Transport, capture and exocytosis of single synaptic vesicles at active zones. *Nature* 406, 849–854
12 Neher, E. (1998) Vesicle pools and Ca^{2+} microdomains: new tools for understanding their roles in neurotransmitter release. *Neuron* 20, 389–399
13 Steyer, J.A. *et al.* (1997) Transport, docking and exocytosis of single secretory granules in live chromaffin cells. *Nature* 388, 474–478
14 Oheim, M. and Stuhmer, W. (2000) Tracking chromaffin granules on their way through the actin cortex. *Eur. Biophys. J.* 29, 67–89
15 Lang, T. *et al.* (1997) Ca^{2+}-triggered peptide secretion in single cells imaged with green fluorescent protein and evanescent-wave microscopy. *Neuron* 18, 857–863
16 Oheim, M. *et al.* (1998) The last few milliseconds in the life of a secretory granule. Docking, dynamics and fusion visualized by total internal reflection fluorescence microscopy (TIRFM). *Eur. Biophys. J.* 27, 83–98
17 Oheim, M. *et al.* (1999) Multiple stimulation-dependent processes regulate the size of the releasable pool of vesicles. *Eur. Biophys. J.* 28, 91–101
18 Han, W. *et al.* (1999) Neuropeptide release by efficient recruitment of diffusing cytoplasmic secretory vesicles. *Proc. Natl. Acad. Sci. U. S. A.* 96, 14577–14582
19 Rohrbach, A. (2000) Observing secretory granules with a multiangle evanescent wave microscope. *Biophys. J.* 78, 2641–2654
20 Tsuboi, T. *et al.* (2000) Simultaneous evanescent wave imaging of insulin vesicle membrane and cargo during a single exocytotic event. *Curr. Biol.* 10, 1307–1310
21 Toomre, D. *et al.* (2000) Fusion of constitutive membrane traffic with the cell surface observed by evanescent wave microscopy. *J. Cell Biol.* 149, 33–40
22 Keller, P. *et al.* (2001) Multicolour imaging of post-Golgi sorting and trafficking in live cells. *Nat. Cell Biol.* 3, 140–149
23 Funatsu, T. *et al.* (1995) Imaging of single fluorescent molecules and individual ATP turnovers by single myosin molecules in aqueous solution. *Nature* 374, 555–559
24 Vale, R.D. *et al.* (1996) Direct observation of single kinesin molecules moving along microtubules. *Nature* 380, 451–453
25 Oiwa, K. *et al.* (2000) Comparative single-molecule and ensemble myosin enzymology: sulfoindocyanine ATP and ADP derivatives. *Biophys. J.* 78, 3048–3071
26 Sako, Y. *et al.* (2000) Single-molecule imaging of EGFR signalling on the surface of living cells. *Nat. Cell Biol.* 2, 168–172
27 Merrifield, C.J. *et al.* (1999) Endocytic vesicles move at the tips of actin tails in cultured mast cells. *Nat. Cell Biol.* 1, 72–74
28 Simons, K. and Toomre, D. (2000) Lipid rafts and signal transduction. *Nat. Rev. Mol. Cell Biol.* 1, 31–39
29 Haugh, J.M. *et al.* (2000) Spatial sensing in fibroblasts mediated by 3′ phosphoinositides. *J. Cell Biol.* 151, 1269–1280